OPTICS

Real-time observation and control of optical chaos

Linran Fan[1]*[†], Xiaodong Yan[2]*, Han Wang[2,3]‡, Lihong V. Wang[1]‡

Optical chaotic system is a central research topic due to its scientific importance and practical relevance in key photonic applications such as laser optics and optical communication. Because of the ultrafast propagation of light, all previous studies on optical chaos are based on either static imaging or spectral measurement, which shows only time-averaged phenomena. The ability to reveal real-time optical chaotic dynamics and, hence, control its behavior is critical to the further understanding and engineering of these systems. Here, we report a real-time spatial-temporal imaging of an optical chaotic system, using compressed ultrafast photography. The time evolution of the system's phase map is imaged without repeating measurement. We also demonstrate the ability to simultaneously control and monitor optical chaotic systems in real time. Our work introduces a new angle to the study of nonrepeatable optical chaos, paving the way for fully understanding and using chaotic systems in various disciplines.

INTRODUCTION

Chaotic behavior is ubiquitous in nature. It has wide and profound influence on many disciplines ranging from fundamental sciences including biology, physics, and mathematics to applications including communication, cryptography, and robotics (1–7). Optical systems have been proven promising for studying chaotic behavior (8–11). Different mechanisms including laser instability (11–13), Kerr nonlinearity (9), and irregular cavities (14, 15) have shown strong chaos. The understanding of these chaotic phenomena in different optical systems is critical to both preventing chaos, when system stability is needed (16), and engineering chaos, when system performance is desired (3, 11, 12). Until now, the study of optical chaotic systems still relies on static imaging (17) and spectral measurement (11, 18). Consequently, only time-averaged effects are revealed, missing critical information about dynamic evolution and sensitivity of optical chaos. The real-time recording of optical chaotic systems has been hindered by the ultrafast movement of photons. Exposure times below picoseconds or imaging speeds above billion frames per second are required. Despite great improvements in the state-of-the-art electronic sensors, these speeds are beyond the capability of current complementary metal-oxide semiconductor and charge-coupled device (CCD) imaging technologies, due to the limited on-chip storage capacity and slow electronic readout speeds (19, 20). Other ultrafast imaging techniques such as Kerr gating have also been developed; however, they normally require repeated measurements under the condition that the chaotic events are highly repeatable (21, 22). The required precise repeatability is in great contradiction to the essence of chaos, which is ultrasensitive to initial conditions and infinitesimal fluctuations, thus nonrepeatable. The lack of ultrafast single-shot detection also limits the capability to control chaotic optical systems, which is highly desired for real applications.
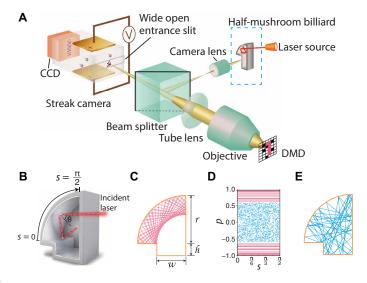
In this study, by reporting a single-shot real-time recording of optical chaotic systems, we demonstrate a possible way to control optical chaos and monitor its dynamics at the same time. Using our compressed ultrafast photography (CUP) technique (23) (Fig. 1A), snapshots of light propagation in two-dimensional (2D) irregular optical cavities are taken at a speed up to 1 billion frames/s. Phase maps of irregular optical cavities are directly measured, which reveals full information of the system. Furthermore, we demonstrate the ability to control and monitor optical chaotic systems in real time by combining the Kerr gate and CUP techniques.

Fig. 1. Schematic of the CUP system and the half-mushroom cavity. (**A**) Schematic setup of the CUP system. Light motions in the half-mushroom cavity are recorded by the CUP system in real time. (**B**) Half-mushroom cavity built from reflective mirrors. The definitions of s and p (= $\sin\theta$) are illustrated. (**C**) Simulated light trajectories in the regular mode. (**D**) The simulated Poincaré surface of section (SOS) phase space of the half-mushroom cavity showing both the regular modes (red lines) and the chaotic modes (blue dots). (**E**) Light trajectories in the chaotic mode.

[1]Caltech Optical Imaging Laboratory, Andrew and Peggy Cherng Department of Medical Engineering and Department of Electrical Engineering, California Institute of Technology, Pasadena, CA 91125, USA. [2]Ming Hsieh Department of Electrical and Computer Engineering, University of Southern California, Los Angeles, CA 90089, USA. [3]Mork Family Department of Chemical Engineering and Materials Science, University of Southern California, Los Angeles, CA 90089, USA.
*These authors contributed equally to this work.
†Present address: James C. Wyant College of Optical Sciences, University of Arizona, Tucson, AZ 85721, USA.
‡Corresponding author. Email: han.wang.4@usc.edu (H.W.); lvw@caltech.edu (L.V.W.)

RESULTS

We first study a 2D half-mushroom cavity, which is a typical cavity structure used in both theoretical and steady-state experimental studies of optical chaos phenomenon (*24–27*). Optical chaotic systems are built on the basis of the classical billiard chaos theory. Light propagation in closed linear 2D cavities with special boundary configurations can show chaotic properties. To characterize the light propagation dynamics, femtosecond laser pulses with 100-fs pulse duration and 800-nm center wavelength from a Ti-sapphire laser are fed into the 2D half-mushroom cavity at a grazing angle (Fig. 1A). The cavity is placed on the imaging plane of the CUP system (*23*). The CUP system is triggered by the Ti-sapphire laser to record the light propagation in the cavity. The total recording time is typically several thousand picoseconds, and the temporal resolution is 10 ps. Weak optical scattering is introduced so the CUP camera can capture motion of light (see Materials and Methods for details).

The half-mushroom cavity, shown in Fig. 1B and fig. S1, is characterized by the radius r of the quarter circle, the foot width w, and foot height h (Fig. 1C). The overall interior surfaces are light reflective and define the half-mushroom cavity boundaries for light propagation. Light propagation inside the cavities can be represented by the reflection position and angle on the quarter circle, which are the Birkhoff coordinates of optical chaotic systems (Fig. 1B). By plotting the Birkhoff coordinates, the Poincaré surface of section (SOS) can be constructed to characterize all system features in phase space (see section S2). In Fig. 1D, we show the simulated SOS of a half-mushroom cavity with $r = 2$ arbitrary units (a.u.), $h = 0.5$ a.u., and $w = 1.2$ a.u. (also see section S3.1). The SOS of the half-mushroom cavity is a mixed phase space, which distinctively shows two regimes: regular and chaotic regimes. In the regular regime, the trajectory of light propagation (Fig. 1C) has a constant reflection angle, showing a horizontal line in SOS. In the chaotic regime, the trajectory of light propagation (Fig. 1E) is ergodic and shows an exponential dependence on initial conditions: incident position described by s and incident angle described by θ (Fig. 1D).

To evaluate how the geometry of the cavity affects and controls its chaotic behavior, a standard half-mushroom cavity (Fig. 2A) and a deformed half-mushroom cavity (Fig. 2B) are built with the only difference being the tilted angle. One trajectory of light propagation inside the standard half-mushroom cavity is shown as time-lapse frames in Fig. 2C and in movie S1. The complete SOS phase map of the half-mushroom cavities is recorded by imaging light propagations under different light incident conditions with the CUP system. The SOS phase map helps us confirm CUP's suitability for the study of optical chaos. After all light trajectories are recorded, the reflection positions and angles on the arc mirror are extracted to form the SOS phase map. For the standard half-mushroom cavity, the SOS phase map is shown in Fig. 2D. Compared to the simulated phase map of a perfect half-mushroom billiard shown in Fig. 1D (also see section S3.1), the sharp boundary between the regular and chaotic regimes disappears. Instead, we observe three types of light propagation in the SOS phase map: (i) Trajectories with $|p| > 0.8$ show small variances in $|p|$ and are similar to those in the regular regime in the perfect half-mushroom cavity (Fig. 1D, red lines); (ii) stable periodic orbits with $0.5 < |p| < 0.8$ are surrounded by invariant curves, which form small islands; and (iii) chaotic trajectories with $|p| < 0.5$ forming the chaotic sea are similar to those in the perfect half-mushroom cavity (Fig. 1D, blue dots). On the basis of the Kolmogorov-Arnol'd-Moser (KAM) theorem

(*28, 29*), such an SOS phase map indicates that the geometry of the standard half-mushroom cavity used in the experiment deviates from the geometry of a perfect half-mushroom cavity (see section S3.2 for the simulated phase map of a half-mushroom cavity with minor deformations). This observation is further confirmed in the deformed half-mushroom cavity by intentionally tilting one mirror to a large angle (Fig. 2B). According to the KAM theorem, larger deformation leads to the disappearance of more invariant curves and to an increase in the chaotic regime. As shown in Fig. 2E, the regular trajectories with large $|p|$ cannot be observed. The SOS phase map mainly consists of chaotic seas with small islands surrounded by invariant curves. The key features in the experimentally obtained phase map in Fig. 2E match well with those in the simulated phase map for this severely tilted half-mushroom cavity (see section S3.3). The above result reveals that cavity geometry is an essential parameter in controlling optical chaos.

Small perturbation in a system can lead to markedly different results, which is the iconic feature of chaotic behavior. In the standard half-mushroom cavity (Fig. 2A), two light trajectories are recorded consecutively with a 1-ms time interval under the same experimental condition. Two such trajectories are shown as time-lapse frames in Fig. 3 (A and B, respectively) (see movie S2). Ideally, these two trajectories should be exactly the same due to the same experimental conditions. Experimental results from Fig. 3 (A and B) show that the two trajectories nearly coincide at the beginning but start to diverge substantially after 900 ps. Time evolution of two trajectories is plotted in SOS phase space in Fig. 3C, which clearly reveals the divergence of two trajectories as time elapses. Figure 3D shows how these two trajectories propagate in the phase space. Although the same experiment conditions are applied to the two light trajectories, the large divergence is due to the infinitesimal drift of the experiment setup over 1 ms. The sensitivity to the initial condition clearly indicates the chaotic behavior of the light propagation. In chaos theory, this behavior belongs to the category of deterministic chaos (*30, 31*), where, due to the extreme sensitivity of the system to the initial condition, small fluctuations in the initial condition make it impossible to predict long-term behavior in general. Any environmental disturbance may drift the experimental setup sufficiently to make the experiment nonrepeatable. This reveals that controlling small perturbation to chaotic system is also key factor to control optical chaos. Comparing to traditional simulation methods or steady-state experimental methods that cannot capture the sensitivity of optical chaos, the unique "one-shot" advantage of CUP becomes critical to studying the chaotic behavior.

We further developed the technique to control and monitor light propagation simultaneously in real time. It is realized with a special cavity design shown in Fig. 4A, which is a quarter Bunimovich stadium (*32, 33*). A successive single-shot light trajectory in Bunimovich stadium is shown in Fig. 4 (A to C) (see the corresponding video data in movie S3). A Kerr gate, consisting of a thin Bismuth Germanate (BGO) crystal and a plate polarizing beam splitter (PBS), is placed at the boundary between the rectangle and quarter-circle parts of the cavity. A Kerr gate can switch the light between regular and chaotic mode. When the Kerr gate is open, light propagation in the quarter Bunimovich stadium always shows chaotic behavior (*32, 33*). When the Kerr gate is closed, light pathways in both the rectangular and quarter-circle cavities separated by the Kerr gate are always nonchaotic (see sections S3 and S4) (*29*). The femtosecond laser at 800-nm center wavelength is first sent into a bulk lithium niobate crystal for frequency
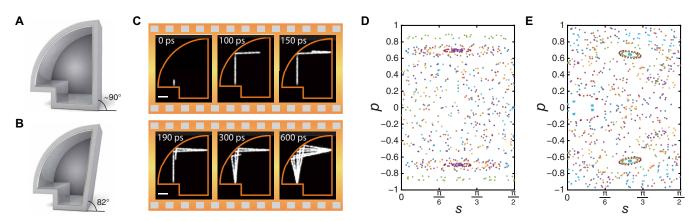
Fig. 2. Single-shot real-time imaging observation of controlling optical chaos by tuning geometry of optical cavities. As-constructed (**A**) regular half-mushroom and (**B**) tilted half-mushroom cavities built from reflective mirrors. (**C**) Time-lapse images showing the light trajectory inside the regular half-mushroom cavity (see corresponding video in movie S1). (**D**) Experimentally obtained Poincaré SOS phase map of the light modes inside the regular half-mushroom cavity in (A). (**E**) Experimentally obtained Poincaré SOS phase map of the light modes inside the tilted half-mushroom cavity in (B).
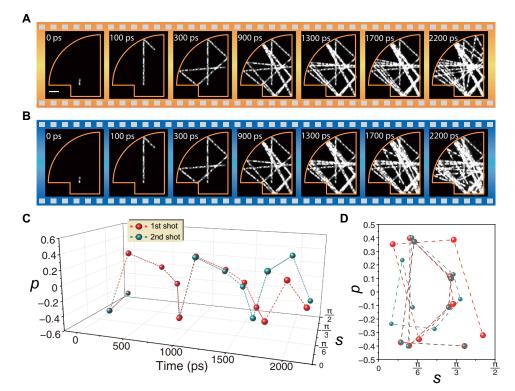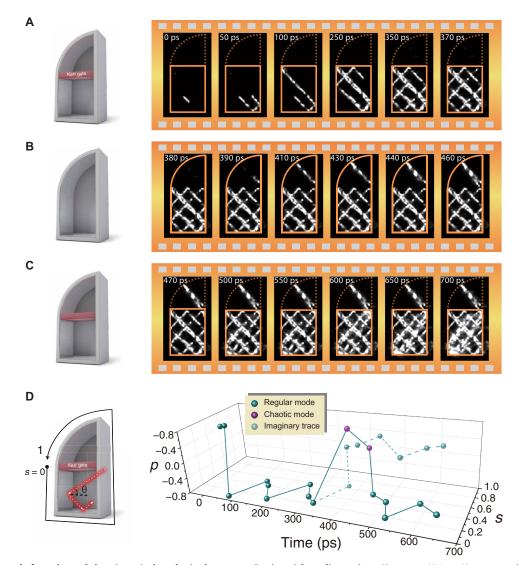

Fig. 3. Single-shot real-time imaging of two light trajectories under the same initial incident conditions. (**A**) Time-lapse images showing the light trajectory inside the half-mushroom cavity. (**B**) Second light trajectory under the same initial incident conditions as that in (A). The corresponding video data showing the temporal evolution of the light pathways in (A) and (B) are provided in the left and middle panels of movie S2, respectively. The right panel of movie S2 shows the combined movie overlaying both light pathways. Infinitesimal differences under the initial condition due to system shift propagates into vastly different light paths as compared to (A). (**C**) Evolution of the light paths in the Poincaré SOS phase spaces over time for the light trajectories in (A) and (B). (**D**) Poincaré SOS phase space shows full trajectories of the two lights.

doubling to 400-nm center wavelength with 10% efficiency. A dichroic mirror is used to separate the 400- and 800-nm optical pulses. The 400-nm pulses are used to probe the light propagation dynamics in the cavity, and the 800-nm pulses are used to control the Kerr gate. A short-pass filter is placed before the CUP system to eliminate the scattered 800-nm light. The polarization of 400-nm

probe light is adjusted to be *s*-polarized, so that light is reflected by the PBS. Therefore, light is confined in the rectangular cavity instead of the quarter Bunimovich stadium (Fig. 4A). The trajectory of light propagation is an invariant curve with constant reflection angles (Fig. 4A). With the 800-nm control light, the 400-nm probe light is changed to *p*-polarization, thus transmitting the PBS (from *t* = 380 ps

Fig. 4. Real-time control of regular and chaotic optical modes in the quarter Bunimovich stadium using a Kerr gate. Using a Kerr gate and a second control light pulse, the light modes can be controlled in real time to transition between regular modes and chaotic modes. Schematic and successive real-time recording of light trajectories inside the quarter Bunimovich stadium when (**A**) the Kerr gate remains closed, (**B**) the Kerr gate remains open from 380 to 470 ps, and (**C**) the Kerr gate remains closed. The corresponding video data showing the temporal evolution of the light pathway in this measurement is provided in movie S3. (**D**) The definitions of s and p (= sinθ) and the experimentally obtained Poincaré SOS phase map corresponding to the light dynamics in (A) to (C) are shown. The regular mode (cyan dot), chaotic mode (purple dot), and predictions of light trajectories if the Kerr gate never opens (light cyan dot) are shown.

in Fig. 4B). The cavity is changed from a rectangle to a quarter Bunimovich stadium, and the light propagation follows a chaotic trajectory instead of the original regular trajectory (Fig. 4B). At t = 470 ps, the Kerr gate is activated again to change the polarization of the 400-nm probe light back to s-polarization (Fig. 4C). Therefore, the probe light is confined in the rectangular cavity again (Fig. 4C). However, the light now propagates in a different regular mode instead of the original regular mode when $t < 380$ ps. This is also shown in the SOS phase space (Fig. 4D). If the Kerr gate never opened, then the light would follow the imaginary trajectory (Fig. 4D, light cyan dots). Instead, because of the switching of the Kerr gate, light trajectory transitioned to the chaotic mode at 390 ps (purple dots) and then transitioned back to a different regular mode after 470 ps (cyan dots).

DISCUSSION
By comparing with traditional time-integrating imaging methods, CUP has great advantages in studying chaos in optical cavities, providing more insights into optical chaos. As chaotic light traverses all spatial points inside the cavity (*25*, *29*), a long-time exposure would overlap the images of the light paths, making it challenging to sort out individual light paths precisely, not to mention quantifying the time sequence of these light paths. The true value of CUP lies in its capability to obtain complete temporal information along with spatial information. One prominent example is to extract the distribution of the Poincaré recurrence time (*34*), which is critical for studying many chaotic cavities (*35*, *36*). In addition, the temporal SOS phase map can reveal the real property of optical cavities if compared with the traditional SOS phase map. It has been found that the traditional

SOS phase map may generate wrong light survival probability in a leaky chaotic limaçon-like cavity as a function of the physical time if compared with the result from a true-time SOS phase map, because a traditional SOS phase map may associate each collision with the same time and may overestimate the collisions that happened within a short period (37). Another example is the dynamic tunneling between regular modes and chaotic modes (27, 38), which can possibly be directly visualized by CUP. It facilitates the study of the dynamic tunneling effect in chaotic cavities and helps in engineering the applications using the tunneling effect (39).

The capability to directly observe and control the optical chaotic behavior in real time in both the spatial and temporal domains opens the door to new research paradigms for optical chaotic systems beyond the traditional theoretical and static experimental approaches. The first-generation CUP system operates at an imaging speed of 100 billion frames/s, with the ability to resolve light dynamics in centimeter-sized optical cavities. CUP systems with an imaging speed of 10 trillion frames/s have already been demonstrated (40), which may allow the ability to resolve light dynamics in integrated nanophotonic cavities. Moreover, by integrating diffraction gratings into CUP systems, the spectral information can also be obtained, which is critical for chaotic systems induced by nonlinear optical processes.

MATERIALS AND METHODS
CUP systems
The operation of the CUP imaging system can be divided into two operational steps: (i) the real-time image acquisition and (ii) the subsequent image reconstruction. In the first step of the measurement, each 2D image frame of the input object video is first projected onto a digital micromirror device (DMD), which encrypts each image with a 2D pseudorandom binary pattern. The encrypted image is then projected onto a stream camera with a widened entrance slit. Within the stream camera, the image is temporally sheared by a sweeping electric field. The resulting sheared image is temporally integrated by a CCD detector array. In the image reconstruction step, the captured data are used to reconstruct the object video based on the encrypted information using compressive sensing algorithms.

The experimental setup is shown schematically in Fig. 1A. The optical cavity is placed at the object plane of the CUP system. To image light propagation, water vapor is used to scatter light into the CUP system. As the streak camera is highly sensitive (single-photon sensitivity in principle), only weak scattering is needed. Therefore, the effects to chaos from these scattering events can be neglected compared with the effects from the deformation of the cavities and opening/closing Kerr gates. The light propagation is first imaged by a 4f system consisting of two lenses with focal lengths of 150 and 25.4 mm, respectively. The intermediate image is then passed to a DMD by another 4f imaging system consisting of a tube lens (focal length, 150 mm) and a microscope objective (focal length, 50 mm; numerical aperture, 0.16). To encode the input image, a pseudorandom binary pattern is generated and displayed on the DMD, with a binned pixel size of 21.6 μm by 21.6 μm (3 3 3 binning). The light reflected from the DMD is collected by the same microscope objective and another tube lens with a focal length of 200 mm and imaged onto the entrance slit of the streak camera. To allow 2D imaging, this entrance slit is opened to its maximal width (~5 mm). Inside the streak camera, a sweeping voltage is applied, deflecting the

encoded image frames according to their times of arrival. The final temporally dispersed image is captured by a CCD with a single exposure.

SUPPLEMENTARY MATERIALS
Supplementary material for this article is available at http://advances.sciencemag.org/cgi/content/full/7/3/eabc8448/DC1

REFERENCES AND NOTES
1. A. Argyris, D. Syvridis, L. Larger, V. Annovazzi-Lodi, P. Colet, I. Fischer, J. García-Ojalvo, C. R. Mirasso, L. Pesquera, K. Alan Shore, Chaos-based communications at high bit rates using commercial fibre-optic links. *Nature* **438**, 343–346 (2005).
2. T. Shinbrot, C. Grebogi, J. A. Yorke, E. Ott, Using small perturbations to control chaos. *Nature* **363**, 411–417 (1993).
3. G. D. Vanwiggeren, R. Roy, Communication with chaotic lasers. *Science* **279**, 1198–1200 (1998).
4. J. P. Gollub, M. Cross, Chaos in space and time. *Nature* **404**, 710–711 (2000).
5. L. Kocarev, S. Lian, *Chaos–Based Cryptography: Theory, Algorithms and Applications* (Springer Science & Business Media, 2011), vol. 354.
6. C. K. Volos, I. M. Kyprianidis, I. N. Stouboulos, A chaotic path planning generator for autonomous mobile robots. *Rob. Auton. Syst.* **60**, 651–656 (2012).
7. A. Uchida, K. Amano, M. Inoue, K. Hirano, S. Naito, H. Someya, I. Oowada, T. Kurashige, M. Shiki, S. Yoshimori, K. Yoshimura, P. Davis, Fast physical random bit generation with chaotic semiconductor lasers. *Nat. Photonics* **2**, 728–732 (2008).
8. J. García-Ojalvo, R. Roy, Spatiotemporal communication with synchronized optical chaos. *Phys. Rev. Lett.* **86**, 5204–5207 (2001).
9. F. Monifi, J. Zhang, Ş. K. Özdemir, B. Peng, Y.-x. Liu, F. Bo, F. Nori, L. Yang, Optomechanically induced stochastic resonance and chaos transfer between optical fields. *Nat. Photonics* **10**, 399–405 (2016).
10. X. Jiang, L. Shao, S.-X. Zhang, X. Yi, J. Wiersig, L. Wang, Q. Gong, M. Lončar, L. Yang, Y.-F. Xiao, Chaos-assisted broadband momentum transformation in optical microresonators. *Science* **358**, 344–347 (2017).
11. M. Sciamanna, K. A. Shore, Physics and applications of laser diode chaos. *Nat. Photonics* **9**, 151–162 (2015).
12. L. Yang, Fighting chaos with chaos in lasers. *Science* **361**, 1201–1201 (2018).
13. N. Bachelard, S. Gigan, X. Noblin, P. Sebbah, Adaptive pumping for spectral control of random lasers. *Nat. Phys.* **10**, 426–431 (2014).
14. I. Favero, K. Karrai, Optomechanics of deformable optical cavities. *Nat. Photonics* **3**, 201–205 (2009).
15. C. Liu, A. Di Falco, D. Molinari, Y. Khan, B. S. Ooi, T. F. Krauss, A. Fratalocchi, Enhanced energy storage in chaotic optical resonators. *Nat. Photonics* **7**, 473–478 (2013).
16. J. Ohtsubo, *Semiconductor Lasers: Stability, Instability and Chaos* (Springer, 2012), vol. 111.
17. M. Plöschner, T. Tyc, T. Čižmár, Seeing through chaos in multimode fibres. *Nat. Photonics* **9**, 529–535 (2015).
18. A. P. Fischer, M. Yousefi, D. Lenstra, M. W. Carter, G. Vemuri, Filtered optical feedback induced frequency dynamics in semiconductor lasers. *Phys. Rev. Lett.* **92**, 023901 (2004).
19. Y. Kondo, K. Takubo, H. Tominaga, R. Hirose, N. Tokuoka, Y. Kawaguchi, Y. Takaie, A. Ozaki, S. Nakaya, F. Yano, T. Daigen, Development of "HyperVision HPV-X" high-speed video camera. *Shimadzu Rev* **69**, 285–291 (2012).
20. M. El-Desouki, M. J. Deen, Q. Fang, L. Liu, F. Tse, D. Armstrong, CMOS image sensors for high speed applications. *Sensors* **9**, 430–444 (2009).
21. A. Velten, T. Willwacher, O. Gupta, A. Veeraraghavan, M. G. Bawendi, R. Raskar, Recovering three-dimensional shape around a corner using ultrafast time-of-flight imaging. *Nat. Commun.* **3**, 745 (2012).
22. L. Wang, P. Ho, C. Liu, G. Zhang, R. Alfano, Ballistic 2-D imaging through scattering walls using an ultrafast optical Kerr gate. *Science* **253**, 769–771 (1991).
23. L. Gao, J. Liang, C. Li, L. V. Wang, Single-shot compressed ultrafast photography at one hundred billion frames per second. *Nature* **516**, 74–77 (2014).
24. J. Andreasen, H. Cao, J. Wiersig, A. E. Motter, Marginally unstable periodic orbits in semiclassical mushroom billiards. *Phys. Rev. Lett.* **103**, 154101 (2009).
25. H. Cao, J. Wiersig, Dielectric microcavities: Model systems for wave chaos and non-Hermitian physics. *Rev. Mod. Phys.* **87**, 61–111 (2015).
26. W. Fang, A. Yamilov, H. Cao, Analysis of high-quality modes in open chaotic microcavities. *Phys. Rev. A* **72**, 023815 (2005).
27. A. Bäcker, R. Ketzmerick, S. Löck, M. Robnik, G. Vidmar, R. Höhmann, U. Kuhl, H.-J. Stöckmann, Dynamical tunneling in mushroom billiards. *Phys. Rev. Lett.* **100**, 174103 (2008).
28. J. U. Nöckel, A. D. Stone, Ray and wave chaos in asymmetric resonant optical cavities. *Nature* **385**, 45–47 (1997).
29. N. Chernov, R. Markarian, *Chaotic Billiards* (American Mathematical Soc., 2006).

30. S. H. Kellert, *In the Wake of Chaos: Unpredictable Order in Dynamical Systems* (University of Chicago Press, 1993).

31. C. Werndl, What are the new implications of chaos for unpredictability? *Br. J. Philos. Sci.* **60**, 195–220 (2009).

32. H. Alt, C. Dembowski, H. D. Gräf, R. Hofferbert, H. Rehfeld, A. Richter, C. Schmit, Experimental versus numerical eigenvalues of a Bunimovich stadium billiard: A comparison. *Phys. Rev. E* **60**, 2851–2857 (1999).

33. P. A. Chinnery, V. F. Humphrey, Experimental visualization of acoustic resonances within a stadium-shaped cavity. *Phys. Rev. E* **53**, 272–276 (1996).

34. N. Haydn, Y. Lacroix, S. Vaienti, Hitting and return times in ergodic dynamical systems. *Ann. Probab.* **33**, 2043–2050 (2005).

35. E. G. Altmann, T. Tél, Poincaré recurrences from the perspective of transient chaos. *Phys. Rev. Lett.* **100**, 174101 (2008).

36. B. V. Chirikov, D. L. Shepelyansky, Correlation properties of dynamical chaos in Hamiltonian systems. *Phys. D Nonlin. Phenom.* **13**, 395–400 (1984).

37. E. G. Altmann, J. S. Portela, T. Tél, Leaking chaotic systems. *Rev. Mod. Phys.* **85**, 869–918 (2013).

38. M. J. Davis, E. J. Heller, Quantum dynamical tunneling in bound states. *J. Chem. Phys.* **75**, 246–254 (1981).

39. Y.-F. Xiao, X.-F. Jiang, Q.-F. Wang, L. Wang, K. Shi, Y. Li, Q. Gong, Tunneling-induced transparency in a chaotic microcavity. *Laser Photon. Rev.* **7**, L51–L54 (2013).

40. J. Liang, L. Zhu, L. V. Wang, Single-shot real-time femtosecond imaging of temporal focusing. *Light Sci. Appl.* **7**, 42 (2018).

Citation: L. Fan, X. Yan, H. Wang, L. V. Wang, Real-time observation and control of optical chaos. *Sci. Adv.* **7**, eabc8448 (2021).

Real-time observation and control of optical chaos

Linran Fan, Xiaodong Yan, Han Wang and Lihong V. Wang

ARTICLE TOOLS	http://advances.sciencemag.org/content/7/3/eabc8448
SUPPLEMENTARY MATERIALS	http://advances.sciencemag.org/content/suppl/2021/01/11/7.3.eabc8448.DC1
REFERENCES	This article cites 36 articles, 4 of which you can access for free http://advances.sciencemag.org/content/7/3/eabc8448#BIBL
PERMISSIONS	http://www.sciencemag.org/help/reprints-and-permissions

Use of this article is subject to the Terms of Service